Development of Ta-Based Superconducting Tunnel Junction X-Ray Detector Arrays

Matthew H. Carpenter, Stephan Friedrich, John A. Hall, Jackson Harris, William K. Warburton, and Robin Cantor

Abstract—We are developing new Ta-based superconducting tunnel junction (STJ) X-ray detectors for high-resolution soft X-ray spectroscopy at synchrotrons. STJ detectors combine the high-energy resolution of cryogenic detectors with the high count rate capabilities of athermal devices and the high efficiencies of solid state detectors, which increases the sensitivity for material analysis by fluorescence-detected X-ray absorption spectroscopy. Our STJ detectors are fabricated using thick, high-Z Ta absorber films that enhance quantum efficiency and spectral purity, and extend operational range to several keV compared with earlier Nb-based STJs. They offer an energy resolution of $\sim$5 to 10 eV FWHM for soft X-rays up to $\sim$1 keV, and count rates of several 1000 counts/s per detector pixel. For increased solid angle coverage, we have fabricated 36- and 112-pixel Ta-based STJ detector arrays with total areas of 1.4 and 4.5 mm^2, respectively. The 208×208 μm^2 pixels have an energy resolution between 6.8 and 7.6 eV FWHM at 525 eV with a low-energy shoulder, and their responsivity is uniform to within 2% across the array. Here we discuss the performance of the array in the context of synchrotron science.

Index Terms—Superconducting photodetectors, superconducting tunnel junctions, synchrotron science, X-ray absorption spectroscopy, X-ray spectroscopy detectors.

I. INTRODUCTION

SUPERCONDUCTING tunnel junctions (STJs) are being developed as X-ray detectors for synchrotron science, because they combine (moderately) high energy resolution, count rate capability and efficiency [1]–[3]. STJs offer an energy resolution between $\sim$2 and $\sim$15 eV FWHM for X-ray energies up to several keV [4]–[8], and can be operated at rates of $\sim$10 000 counts/s per detector pixel [3], [9], [10]. For synchrotron science applications, they can increase the sensitivity of fluorescence-detected X-ray absorption spectroscopy (XAS) whenever semiconductor X-ray detectors lack energy resolution and grating spectrometers lack the efficiency to detect a weak X-ray signal close to a stronger X-ray emission line

[3], [11]. At synchrotrons, STJ X-ray detectors are therefore most commonly used for chemical analysis of dilute samples in the energy range below $\sim$1 keV where characteristic X-ray lines often have energies separated by only $\sim$10 to $\sim$50 eV [12]–[14].

While Ta-based STJs with imaging capabilities have been developed for astronomy applications for over a decade [7], STJs for synchrotron science have so far relied on Nb-based detectors [3], [8], [9], [12]–[14], because here large junction areas and simple readout are more important than highest energy resolution and imaging capabilities [11], and Nb-STJs with these properties had been the most advanced until now. We have recently begun to develop Ta-based STJs optimized for synchrotron science [10] in order to:

- utilize the higher absorption efficiency of Ta over Nb,
- reduce the line-splitting artifact from photon absorption in the STJ's bottom electrode,
- extend STJ operation at synchrotrons from currently $\sim$1 keV to several keV,
- and (less relevant here) to attain higher energy resolution.

Here we present the first X-ray spectra of the Ta-STJ arrays we have built and discuss the performance of these devices.

II. EXPERIMENTAL SETUP

A. STJ Operating Principle

STJ X-ray detectors consist of two superconducting electrodes separated by a thin tunnel barrier. X-ray absorption in one of the junction electrodes creates excess quasiparticles in proportion to the X-ray energy, and the resulting increase in tunneling current can be read out directly with a room temperature amplifier. For increased efficiency, each electrode typically consists of a thick large-gap absorber (Nb or Ta) and a lower-gap trap (Al) to confine the excess quasiparticles close to the junction barrier and speed up tunneling. The limiting energy resolution of STJs is set to a few eV by the statistics of the charge generation and tunneling processes, and the maximum detector speed is determined by the excess quasiparticle life time in the junction electrodes.

B. Fabrication of Devices

The Ta-based STJ detectors described here consist of Nb/Ta/Al/AlOx/Al/Ta multilayers sputter-deposited in a single vacuum cycle on standard 100-mm diameter oxidized Si wafers and patterned photolithographically. Details of the fabrication process will be described elsewhere. The Ta films serve as
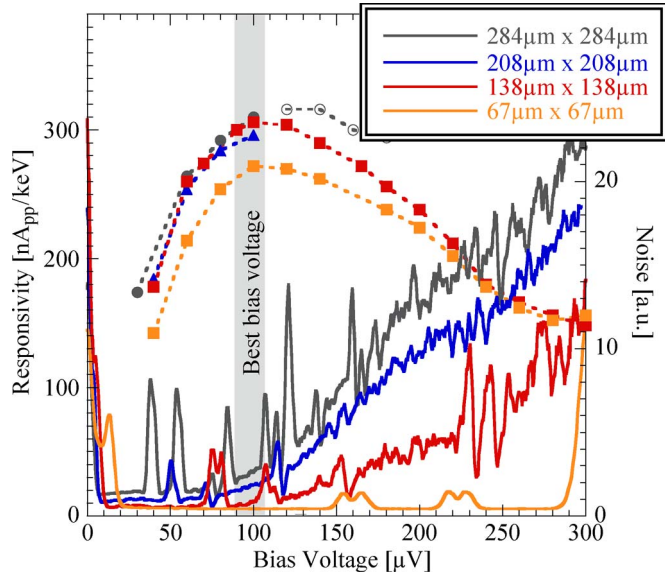
Fig. 1. Responsivity and baseline noise for Ta-STJs of different size. All devices have a low-noise region between Fiske mode resonances at $\sim 100\ \mu\text{V}$ for biasing at a voltage where the responsivity is high. Results are from single devices and are typical of devices of their size.

absorbers, with a thin (~ 5 nm) Nb layer underneath the bottom electrode to nucleate Ta film growth in the desired bcc phase with $\Delta_{\text{Ta}} \approx 0.7$ meV. The bottom Ta electrode thickness is 265 nm, and devices with top Ta electrodes ranging in thickness from 165 nm to 500 nm have successfully been fabricated. Thick top Ta electrodes are desirable to reduce the line splitting artifact caused by X-ray absorption in the bottom Ta electrode. The AlOx barrier thickness is adjusted to achieve a critical current density of ~ 150 A/cm^2.

C. Detector Testing

The detectors were operated in a two-stage adiabatic demagnetization refrigerator inside a cryoperm magnetic shield at an unregulated temperature of ~ 0.1 K. A magnetic field of ~ 5 mT was applied along the junction diagonal to reduce the dc Josephson current and suppress the Fiske mode resonances.

The STJs were illuminated with X-rays from a two-stage Henke-type generator with a primary tungsten/tantalum target that illuminates different secondary target samples on a rotatable target wheel. X-ray-induced pulses were processed in two ways. Signals were either amplified with a manual current-sensitive single-channel preamplifier [15] and stored for subsequent digital analysis, or they were amplified by a prototype 32-channel computer-controlled preamplifier and processed in real time by a trapezoidal filter implemented in a FPGA [16]. When fully developed, this 32-channel board by XIA LLC will be available for commercial STJ X-ray spectrometers.

III. SINGLE PIXEL STJ CHARACTERIZATION

For testing purposes we typically fabricate both single-pixel STJs and detector arrays on the same wafer. Fig. 1 shows the responsivity and noise characteristics for square STJs of different size as a function of bias voltage. The signal increases with increasing voltage up to a maximum around $\sim 100\ \mu\text{V}$ as
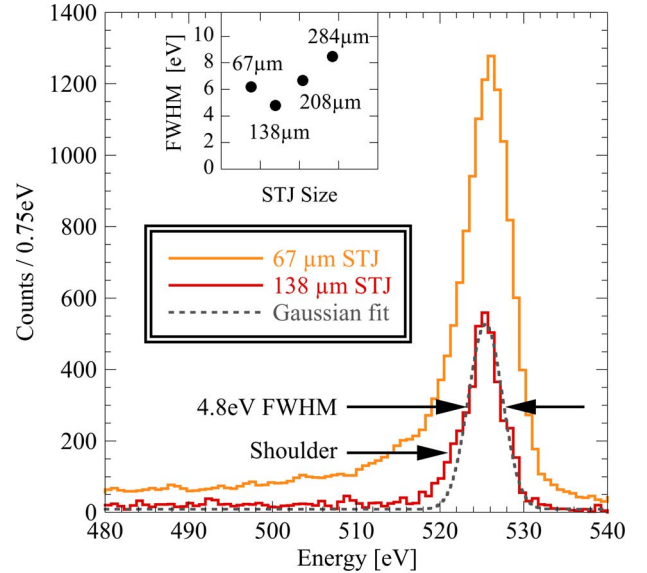

Fig. 2. Low-energy response of Ta-STJs of different size. The inset shows the energy resolution for oxygen K X-rays at 525 eV.

tunneling against the bias is suppressed. At higher voltages, the signal decreases because quasiparticles enter the counterelectrode at an energy above the Ta gap so that they are less likely to be confined in the Al trap [10]. Due to their high capacitance, signals from the large $(284\ \mu\text{m})^2$ STJs exhibit a slight overshoot for voltages $> 100\ \mu\text{V}$ that makes the peak height appear artificially high (open circles). The devices have similar responsivities, except for the smallest one with an area of $(67\ \mu\text{m})^2$ (solid squares). This suggests that the quasiparticle lifetime is set by STJ edges, but this edge loss is not very strong since it no longer changes once the detector dimensions exceed $\sim 100\ \mu\text{m}$.

The STJ noise in Fig. 1 is a measurement of the rms fluctuations at each bias point over the entire bandwidth of the preamplifier. The noise depends on the leakage current and the voltage noise of the FET at the preamplifier input, and thus changes with dynamic resistance. It therefore increases for increasing junction area due to higher leakage current and reduced dynamic resistance. In addition, the noise peaks at the voltages of the Fiske mode resonances where the dynamic resistance is reduced. In the smaller devices with wider Fiske modes, the noise peaks are split due to the higher dynamic resistance at the peak of the resonance [10].

Fig. 2 shows the energy resolution of the different devices at the oxygen K line at 525 eV. Interestingly, the best energy resolution of 4.8 eV FWHM is observed for the $(138\ \mu\text{m})^2$ STJ, although the baseline noise of the smaller $(67\ \mu\text{m})^2$ STJ is lower. This suggests that the electronic noise does not contribute significantly to the broadening of the line. This agrees with a measured electronic pulser width between 2 and 3 eV FWHM. Interestingly, the observed energy resolution is always better at the oxygen K line than at the lower-energy nitrogen K, carbon K and boron K lines, whose resolution tends to be ~ 2 to ~ 3 eV worse. This cannot be explained by electronic or statistical noise, nor by spatial inhomogeneities in the detector response. The lower energy resolution of these lines is likely not limited by the device performance, but rather
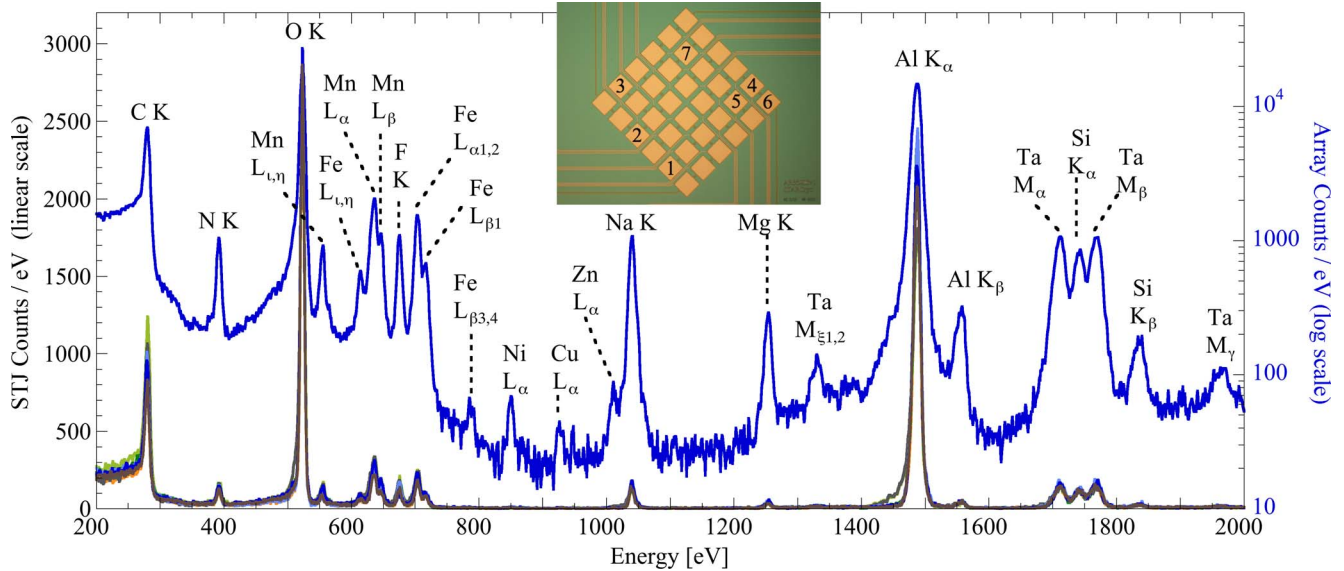
Fig. 3. Low energy X-ray response of seven individual STJs in the 36-pixel array (linear scale), and the sum spectrum on a log scale. Note the detection of the weak Fe $L_{\beta 3,4}$ and Ni L_α lines when several spectra are added. The inset shows which seven pixels of the array were used.

by line broadening from the source. This may either be due to the presence of multiple chemical forms of the same elements, possibly due to oxidation or water absorption, each with a centroid at a slightly different energy. It may also be due to the intrinsic width of the electronic band that gives rise to the X-ray transition.

We also observe a low-energy shoulder on the O K peaks in Fig. 2. It is more pronounced for the smaller devices, which suggests that it is due to quasiparticle losses at the edges of the STJ. We therefore do not use the spectrum below the halfway point on the low-energy side of each peak for the Gaussian fit to extract the energy resolution.

IV. STJ ARRAY CHARACTERIZATION

A. Individual STJ Readout

To test the homogeneity of the response across an array, we have exposed eight STJs from a 36-pixel array with 165 nm top Ta electrode to radiation from an $MnO + Fe_7(CN)_{18}$ powder sample taped to an Al sample holder at a low count rate of $\sim$100 Hz/pixel limited by the X-ray source brightness. One STJ had an open circuit due to a mask defect which has since been corrected, and the response of the other seven were recorded one at a time with a single-channel current-sensitive preamplifier. The signal pulses were written to disc and processed with a 6 μs Gaussian filter. For energies above $\sim$1 keV, the fraction of the incident X-rays absorbed in the base layer gives rise to a line splitting artifact, which was removed by rise time discrimination.

At a bias voltage of 100 μV, the STJs had a responsivity of 285 ± 1.9 nA$_{pp}$/keV, and the maximum variation between pixels was 2%. While this is very uniform, it still requires that each pixel be calibrated individually. We have also observed a small non-linearity in the response, and calibrated the energy scale with a quadratic function to the peak values of the C K, O K, Fe $L_{\alpha 1}$, Na K, Al K_α and Si K_α lines.

Fig. 3 shows the response of the seven individual pixels on a linear scale, plus the sum spectrum on a logarithmic scale. The resolution at the oxygen K line at 525 eV varies between 6.8 and 7.6 eV FWHM for the seven individual STJs, and is 7.2 eV for the sum spectrum. The peak to background ratio is limited by inelastic scattering of the bremsstrahlung from the primary X-ray target. Still, it is sufficiently high that even the weak Fe $L_{\beta 3,4}$ line at 792 eV and the Zn $L_{\alpha 1}$ line at 1012 eV from the $\sim$0.25% Zn in the Al-6061 holder underneath the sample and the carbon tape are visible. This combination of energy resolution and uniformity is sufficient for most fluorescence XAS applications at synchrotrons where the primary requirement for the X-ray detector is the ability to separate different X-ray lines efficiently.

B. Readout With Shared Ground Return

For the operation of STJ arrays at a synchrotron, it is of course essential to operate all pixels simultaneously. In addition, it is desirable to use as few wires as possible to minimize the heat load into the cold stage. In the past, we have therefore operated nine Nb-STJ pixels with a single ground return wire [12]–[14]. We have similarly designed the current Ta-STJ arrays such that nine STJs share the same $\sim$10 Ω ground wire, as shown in the inset in Fig. 3. With Ta-STJs demonstrating better energy resolution than the earlier Nb-STJ, we have examined whether crosstalk might affect array performance or limit the number of STJs that can share a single ground wire. These measurements also allowed testing of the 32-channel STJ preamplifier prototype that is currently being developed at XIA.

We have biased one of the high-resolution STJs at 100 μV with the new computer-controlled array preamplifier, and exposed it to radiation from the $MnO + Fe_7(CN)_{18}$ sample on the Al holder. The resolution was 6.8 eV FWHM as it had been with the earlier amplifier, indicating that electronic noise does not dominate the detector resolution. We have then successively
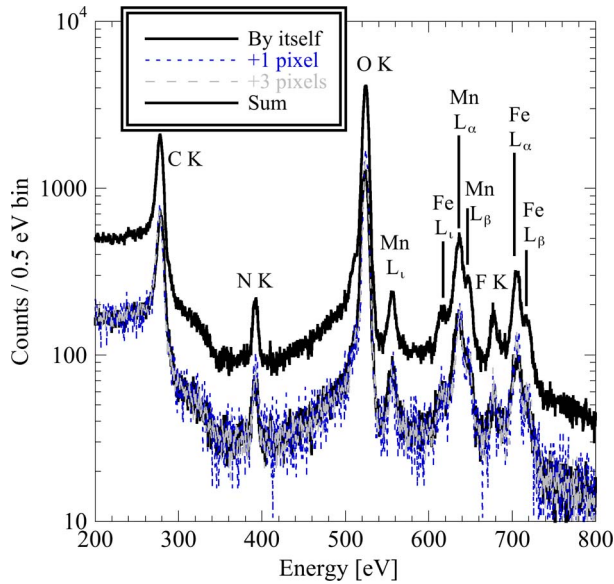
Fig. 4. Low-energy X-ray spectrum of the same $(208 \; \mu\text{m})^2$ STJ when sharing the ground wire with 0, 1, and 3 other STJs in the 36-pixel array. The three individual pixel spectra are plotted on top of one another.

added additional pixels that share the same ground wire and measured the spectra simultaneously.

Fig. 4 shows the low-energy response of the same detector when sharing the same ground wire with zero, one, or three other STJs, normalized to the same data acquisition time of 1 hour. (Our current digital preamplifier backplane only supports up to four pixels simultaneously.) The resolution at O K is degrading slightly from initially 6.8 eV to 6.9 and 7.1 eV FWHM as more pixels are added. While this might indicate some cross talk, this variation is close to the ± 0.1 eV error of the measurement. This indicates that, if there is in fact any crosstalk, it is very small and clearly does not preclude the operation of Ta-STJ arrays with shared ground wires at synchrotrons.

V. CONCLUSION

We have built 36-pixel arrays of Ta-based STJ detectors for X-ray spectroscopy at synchrotrons. We have demonstrated an energy resolution between 6.8 and 7.6 eV FWHM at 525 eV for $(200 \; \mu\text{m})^2$ STJ pixels whose response is sufficiently uniform to allow scaling to large array sizes. The resolution is as high as 4.8 eV FWHM in $(138 \; \mu\text{m})^2$ STJs. This resolution allows full separation of emission lines from different elements which, combined with the increased solid angle coverage of large

arrays, promises increased sensitivity for fluorescence-detected XAS. We are currently integrating these arrays into a complete soft X-ray spectrometer for synchrotron science.

REFERENCES

[1] "For an overview of current cryogenic detector performance," *J. Low Temp. Phys.*, vol. 167, 2012.

[2] "For an overview of current cryogenic detector performance," presented at the Proc. 14th Int. Workshop LTD.

[3] S. Friedrich, "Cryogenic X-ray detectors for synchrotron science," *J. Synch. Rad.*, vol. 13, pp. 159–171, 2006.

[4] J. B. LeGrand, C. A. Mears, L. J. Hiller, M. Frank, S. E. Labov, H. Netel, D. Chow, S. Friedrich, and M. A. Lindeman, "A superconducting tunnel junction X-ray detector with performance limited by statistical effects," *Appl. Phys. Lett.*, vol. 73, pp. 1295–1297, 1998.

[5] G. Angloher, P. Hettl, M. Huber, J. Jochum, F. V. Feilitzsch, and R. L. Möss-bauer, "Energy resolution of 12 eV at 5.9 keV from Al-superconducting tunnel junction detectors," *J. Appl. Phys.*, vol. 89, pp. 1425–1427, 2001.

[6] L. Li, L. Frunzio, C. Wilson, D. E. Prober, A. E. Szymkowiak, and S. H. Moseley, "Improved energy resolution of x-ray single photon imaging spectrometers using superconducting tunnel junctions," *J. Appl. Phys.*, vol. 90, pp. 3645–3646, 2001.

[7] P. Verhoeve, "Photon counting low temperature detectors for visible to gamma ray astrophysics," *J. Low Temp. Phys.*, vol. 151, pp. 675–683, 2008.

[8] S. Shiki, M. Ukibe, Y. Kitajima, and M. Ohkubo, "X-ray detection performance of 100-pixel superconducting tunnel junction array detector in the soft X-ray region," *J. Low Temp. Phys.*, vol. 167, pp. 748–753, 2012.

[9] M. Frank, L. J. Hiller, J. B. le Grand, C. A. Mears, S. E. Labov, M. A. Lindeman, H. Netel, D. Chow, and A. T. Barfknecht, "Energy resolution and high count rate performance of superconducting tunnel junction x-ray spectrometers," *Rev. Sci. Instrum.*, vol. 69, pp. 25–31, 1998.

[10] S. Friedrich, M. H. Carpenter, O. B. Drury, W. K. Warburton, J. Harris, J. Hall, and R. Cantor, "New developments in superconducting tunnel junction X-ray spectrometers for synchrotron science," *J. Low Temp. Phys.*, vol. 167, pp. 741–747, 2012.

[11] O. B. Drury and S. Friedrich, "Sensitivity and S/N-ratio of superconducting high-resolution X-ray spectrometers," *IEEE Trans. Appl. Supercond.*, vol. 15, pp. 613–617, 2005.

[12] P. Fons, H. Tampo, A. V. Kolobov, M. Ohkubo, S. Niki, J. Tominaga, R. Carboni, F. Boscherini, and S. Friedrich, "Direct observation of nitrogen location in molecular beam epitaxy grown nitrogen-doped ZnO," *Phys. Rev. Lett.*, vol. 96, p. 045504, 2006.

[13] K. Ndung'u, S. Friedrich, A. R. Gonzalez, and A. R. Flegal, "Chromium oxidation by manganese (hydr)oxides in a California aquifer," *Appl. Geochem.*, vol. 25, pp. 377–381, 2010.

[14] M. Zhuravleva, S. Friedrich, and C. L. Melcher, "Praseodymium valence determination in Lu_2SiO_5, Y_2SiO_5, and $Lu_3Al_5O_{12}$ scintillators by X-ray absorption spectroscopy," *Appl. Phys. Lett.*, vol. 101, p. 101 902, 2012.

[15] S. Friedrich, K. Segall, M. C. Gaidis, C. M. Wilson, D. E. Prober, P. J. Kindlmann, A. Szymkowiak, and S. H. Moseley, "Single photon imaging X-ray spectrometers using low noise current preamplifiers with DC voltage bias," *IEEE Trans. Appl. Supercond.*, vol. 7, pp. 3383–3386, 1997.

[16] W. K. Warburton, J. Harris, M. Carpenter, P. M. Grudberg, L. Fabris, and S. Friedrich, "Preamplifier development for superconducting tunnel junction array detector electronics," presented at the Conf. Rec. IEEE Nucl. Sci. Symp., Knoxville, TN, 2010.